PRAMANA — journal of physics

Vol. 82, No. 5
May 2014
pp. 789–795

Double folding model analysis of elastic scattering of halo nucleus ^{11}Be from ^{64}Zn

M HEMALATHA
UM–DAE Centre for Excellence in Basic Sciences, Mumbai 400 098, India
E-mail: hema@cbs.ac.in

DOI: 10.1007/s12043-014-0729-2; ***e*Publication:** 17 April 2014

Abstract. Calculations of elastic scattering cross-sections for ^{9,10,11}Be + ^{64}Zn at near-Coulomb barrier energy have been performed using a potential obtained from the double folding model and are compared with the experiment. In the framework of the double folding model, the nuclear matter densities of ^{9,10,11}Be projectiles and a ^{64}Zn target are folded with the complex energy-dependent effective M3Y interaction. The angular distributions of the differential cross-section for ^{9,10}Be scattering from ^{64}Zn at $E_{\text{c.m.}} \approx 24.5$ MeV agree remarkably well with the data, while in case of ^{11}Be, calculations show a Coulomb–nuclear interference peak which is not observed in the data.

Keywords. Halo nuclei; elastic scattering; double folding model.

PACS Nos 24.10.Ht; 25.60.–t; 25.60.Bx; 25.60.Dz

1. Introduction

With the continuous advancement of radioactive ion beam facilities worldwide, accelerated radioactive beams including halo nuclei have become accessible for investigation. The nuclei such as ^{11}Be (one-neutron halo), ^{6}He and ^{11}Li (two-neutron halo), in contrast to stable nuclei, have distinct features such as extended neutron density distribution and a compact core. In addition, some very neutron-rich nuclei exhibit astonishingly large matter radii in comparison with neighbouring nuclei [1,2]. The halo structure observed in some of the loosely bound nuclei arises due to the low binding energy of the last nucleons. The outer neutrons have a high probability of being present at a large distance from the core, where the nuclear interaction is quite weak. The core remains almost unperturbed by the presence of the halo, and exhibits the usual characteristics. The unusual features of halo nuclei largely affect the interaction with light and heavy targets at low bombarding energies and have created tremendous interest in the study of nuclear reactions. Elastic scattering is sensitive to the nature of the surface of nuclei and hence it is effective in studying halo nuclei.

When two 'normal' nuclei collide, as the short-range nuclear interaction takes over, the system moves away from the elastic channel due to non-elastic processes and the elastic cross-section decreases. The resulting angular distribution has a Fresnel diffraction form with analogy to that in optics. These nuclei show strong absorption angular distributions varying from Fresnel-type at energies near the Coulomb barrier to oscillatory Fraunhofer-type at energies well above the barrier. The elastic scattering angular distribution may also show a peak due to a balance of nuclear and Coulomb forces in analogy with the Coulomb rainbow model. The 'normal' nuclei, in general, show either of the classical diffraction patterns. However, the elastic scattering angular distribution of neutron halo nuclei scattering from heavy targets at near-barrier energies are very different from stable, tightly bound nuclei. In the scattering with heavy targets at low energies, the combination of the nuclear interaction and the strong electric field makes the core and the halo neutrons move in opposite directions, thus, producing strong coupling to dipole modes of the system at relatively low excitation energy. In halo nuclei, these effects of dipole polarizibility are important and it affects the elastic scattering cross-section [3].

Experiments of the scattering of halo nuclei with light and heavy targets are being carried out which provide valuable insight for improving our understanding of nuclear reactions. One of the interesting aspects is to understand the effect of the halo structure, on elastic scattering cross-sections at near-Coulomb barrier energies in reactions induced by neutron halo nuclei and weakly bound radioactive beams. A number of detailed experimental studies have been carried out so far, for the case of light neutron halo systems like ^{6}He, ^{11}Li and ^{11}Be [4–7].

The structures exhibited by the three isotopes of beryllium under consideration (^{9,10,11}Be) are very different. ^{11}Be is the archetypal one-neutron halo nucleus. The ground and first excited states both have halo structure, in which the outermost neutron is extremely weakly bound and the ground state has positive parity. The isotope ^{10}Be is even–even, with large one-neutron separation energy. The α–α clusterization continues in this nucleus. The considerably larger binding energy resulting by the addition of a neutron to ^{9}Be is due to enhanced pairing. The isotope ^{9}Be is the only stable one, and it retains the highly deformed double-α shape, due to the proximity of the low-lying $2\alpha 1n$ threshold. It is a weakly-bound Borromean nucleus, i.e., three separate particles of the nucleus are bound together in such a way that if any one is removed, the remaining two become unbound, just like the rings of the Borromean family crest. The one-neutron separation energies [8] for ^{9,10,11}Be are 1664.54 $\pm$ 0.10 keV, 6812.28 $\pm$ 0.09 keV and 501.64 $\pm$ 0.25 keV, respectively. The next section describes the double folding model, and reaction cross-sections are calculated within this framework.

2. Double folding model

In double folding (DF) model, the real nucleus–nucleus optical potential is given by the expression [9]

$$V^{\mathrm{DF}}(r) = \int \mathrm{d}r_1 \int \mathrm{d}r_2 \rho_1(r_1)\rho_2(r_2)v_{\mathrm{nn}}(s), \tag{1}$$

where $\rho_1(r_1)$ and $\rho_2(r_2)$ are the nuclear matter density distributions for the two interacting nuclei, respectively, and $v_{\mathrm{nn}}(s)$ is the effective nucleon–nucleon (NN) interaction with

$s = |r - r_1 + r_2|$ as the distance between the two nucleons. As there is integration over two densities, this is called the DF model.

The M3Y *NN* interaction used is the one prescribed by Bertsch *et al* [10], which is expressed as a sum of three Yukawa terms. It is obtained from the fitting of the *G*-matrix element based on the Reid–Elliot *NN* interaction. The explicit form of the M3Y interaction is given as

$$v_{\rm nn}(s) = 7999\frac{{\rm e}^{-4s}}{4s} - 2134\frac{{\rm e}^{-2.5s}}{2.5s} + J_{00}(E)\delta(s), \tag{2}$$

where the zero-range pseudopotential $J_{00}(E)$ represents the single-nucleon exchange term and is given by [9]

$$J_{00}(E) = -276(1 - 0.005E/A)\ {\rm MeV\,fm}^3, \tag{3}$$

where E and A are the incident energy and mass number of the projectile, respectively. $J_{00}(E)$ imparts a very weak energy dependence on the folded potential.

2.1 *Nuclear matter densities*

The one-neutron halo nucleus ^{11}Be is considered to be composed of a ^{10}Be core and one neutron as

$$\rho_{^{11}{\rm Be}}(r) = \rho_{^{10}{\rm Be}}(r) + \rho_{\rm n}(r). \tag{4}$$

The density of the ^{10}Be core is considered to have a Fermi form [11] with root-mean-square (rms) matter radius of 2.30 fm [12].

$$\rho_{^{10}{\rm Be}}(r) = \frac{\rho_0}{1 + \exp(r - R)/a}, \tag{5}$$

where ρ_0 can be determined from the normalization condition

$$4\pi \int \rho(r) r^2 {\rm d}r = 10. \tag{6}$$

The density of the one-neutron halo is ascribed a Gaussian form [13] and the parameters of this density are adjusted to obtain rms matter radius of 2.73 fm [12] for ^{11}Be.

$$\rho_{\rm n}(r) = (a\sqrt{\pi})^{-3}\exp\left(-\frac{r^2}{a^2}\right). \tag{7}$$

For consistency, the density of ^{9}Be is independently assumed to have a Fermi form as in eq. (5) with rms charge radius of 2.519 fm [14].

The ^{64}Zn nuclear charge densities are taken in the Fermi form as given by eq. (5) with the parameters from [14].

The nuclear matter densities required for the calculation of DF potential were obtained from the available nuclear charge radius in case of ^{9}Be and ^{64}Zn, using the code DFPOT, the details of which are given in [15].

3. Results and discussion

3.1 *Double folded potential*

The real and the imaginary parts of the potential are calculated using DF model, employing the M3Y effective *NN* interaction and the densities. It is known that, the real part of the potential can be determined phenomenologically or microscopically without much ambiguity whereas, the imaginary part is somewhat deficient. Alternatively, one may choose the imaginary part of the optical model potential (OMP) phenomenologically to be consistent with the experimental data. In the present analysis, the imaginary part of the potential is assumed to be the same as the real part of the double folded potential but with a different renormalization constant. The spin-orbit part of the potential is not considered as it has only a small effect on the calculated cross-sections. The double folded potential is thus expressed as

$$U^{\mathrm{DF}}(r) = (N_V + iN_W)V^{\mathrm{DF}}(r) + U_{\mathrm{C}}(r), \tag{8}$$

where N_V and N_W are the renormalization constants of the real and imaginary microscopic potentials, respectively. V^{DF} is the folded potential that is calculated with density-

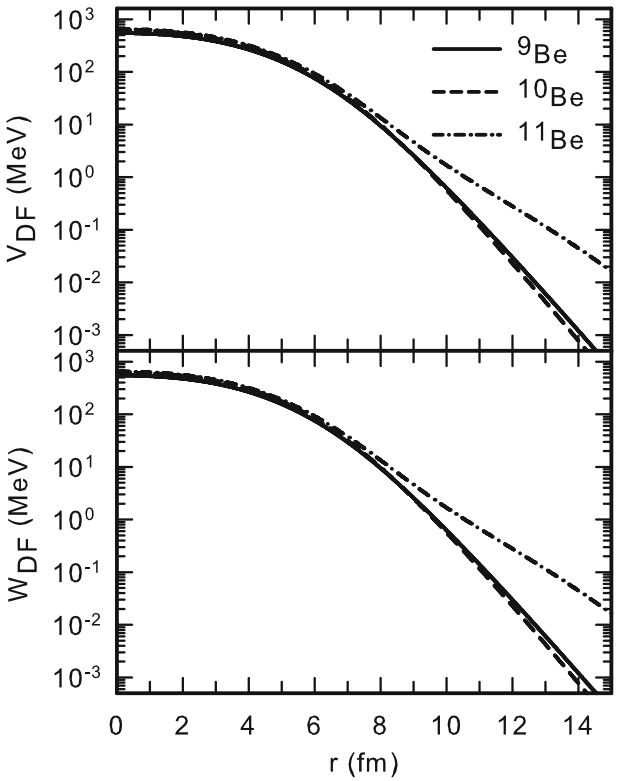

Figure 1. The real (V_{DF}) and the imaginary (W_{DF}) parts of the potential for ^{9,10,11}Be, calculated using DF model.

independent M3Y effective *NN* interaction. The Coulomb potential $U_C(r)$ is taken as the usual Coulomb form between a point charge and a uniform charge distribution of radius

$$R_c = r_c \left(A_P^{1/3} + A_T^{1/3} \right) \tag{9}$$

with $r_c = 1.3$ fm.

The calculated real and imaginary folded potentials with the renormalization constants (N_V and N_W, respectively) as unity, for ^{9,10,11}Be projectiles scattering from ^{64}Zn target, as a function of the radial distance r, are shown in figure 1.

To minimize the number of parameters, renormalization N_V for the real part of the DF potential was fixed at unity and a search was carried out on N_W to achieve a minimum χ^2 to fit the differential cross-section data. The values of the fit obtained in this manner along with the χ^2 values for the differential cross-section and reaction cross-section σ_R for ^{9,10,11}Be are listed in table 1. The final real and imaginary parts of the potentials are then obtained by multiplying the potential by the corresponding renormalization constant.

3.2 *Cross-sections*

The differential and total reaction cross-sections, similar to [16] have been computed and the effect of an additional neutron in Be projectile scattering of ^{64}Zn target, on the angular distributions have been investigated in terms of the DF model. The real and the imaginary parts of the DF potential were used in the code ECIS94 [17] to obtain the differential and the total reaction cross-sections. The angular distributions of ^{9,10,11}Be + ^{64}Zn elastic scattering cross-section at $E_{c.m.} \approx 24.5$ MeV are presented in figure 2. Clearly, the DF calculations reproduce the peak due to Coulomb–nuclear interference that is observed in the corresponding data [6] for ^{9,10}Be. For ^{11}Be, the calculations show Coulomb–nuclear interference peak (CNIP) that is not observed in the corresponding data. Calculations incorporating dynamic polarization potential (DPP) are in progress, and these are expected to explain the absence of CNIP in the ^{11}Be data.

Table 1. Normalization parameters for the real, N_V, and imaginary, N_W, parts of the DF potential for elastic cross-sections, chi-square (χ^2) values for the differential and reaction cross-sections (σ_R).

	N_V	N_W	χ^2/N	σ_R (mb)
^{9}Be + ^{64}Zn	1.00	0.94	1.0	1112
^{10}Be + ^{64}Zn	1.00	1.10	12.1	1244
^{11}Be + ^{64}Zn	1.00	1.00	48.6	1854

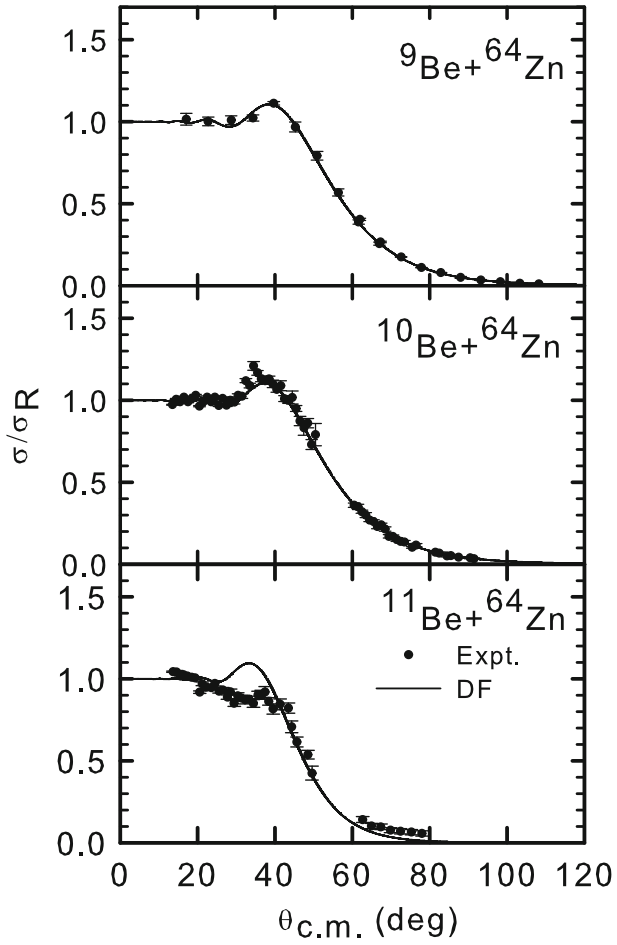

Figure 2. The ratio to Rutherford cross-section for ^{9,10,11}Be scattering from ^{64}Zn at $E_{\text{c.m.}} \approx 24.5$ MeV. The dots are the experimental values taken from [6] while the solid line corresponds to the DF calculations.

4. Conclusions

Elastic scattering of light halo nuclei from a variety of heavier systems provides rich insights into the understanding of both nuclear reactions and structure. Recently, there have been many experimental and theoretical investigations focussed on this aspect. In the present work, calculations have been performed for the elastic scattering cross-sections of Be isotopes ^{9,10,11}Be on ^{64}Zn at a near-Coulomb barrier energy. These calculations utilize potential from the DF model. The double folded potential is obtained by folding the nuclear matter densities of ^{9,10,11}Be projectiles and ^{64}Zn target with the complex energy-dependent effective M3Y interaction. For the isotopes ^{9,10}Be which do not have a halo structure, the angular distributions of the differential cross-section for scattering from ^{64}Zn at $E_{\text{c.m.}} \approx 24.5$ MeV are in good agreement with experimental

measurements. For ^{11}Be, which has a halo structure, experimental data indicate suppression of the Coulomb–nuclear interference peak. The present calculations do not reproduce this trend, but it is expected that calculations including a dynamic polarization potential, which are in progress, will better explain the observations.

References

[1] I Tanihata *et al*, *Phys. Lett. B* **160**, 380 (1985)
[2] I Tanihata *et al*, *Phys. Rev. Lett.* **55**, 2676 (1985)
[3] M V Andres *et al*, *Phys. Rev. Lett.* **82**, 1387 (1999)
[4] L F Canto *et al*, *Phys. Rep.* **424**, 1 (2006)
[5] N Keeley *et al*, *Prog. Part. Nucl. Phys.* **63**, 396 (2009)
[6] A Di Pietro *et al*, *Phys. Rev. Lett.* **105**, 022701 (2010)
[7] M Cubero *et al*, *Phys. Rev. Lett.* **109**, 262701 (2012)
[8] M Wang *et al*, *Chin. Phys. C* **36**, 1603 (2012)
[9] G R Satchler and W G Love, *Phys. Rep.* **55**, 183 (1979)
[10] G F Bertsch, J Borysowicz, H McManus and W G Love, *Nucl. Phys. A* **284**, 399 (1977)
[11] R E Warner *et al*, *Phys. Rev. C* **54**, 1700 (1996)
[12] I Tanihata *et al*, *Phys. Lett. B* **206**, 592 (1988)
[13] A K Chaudhuri, *Phys. Rev. C* **49**, 1603 (1994)
[14] H De Vries, C W De Jager and C De Vries, *At. Data Nucl. Data Tables* **36**, 495 (1987)
[15] J Cook, *Comput. Phys. Commun.* **25**, 125 (1982)
[16] M Hemalatha *et al*, *Phys. Rev. C* **70**, 044320 (2004)
[17] J Raynal, CEA Report No. CEA-N-2772 (1994)